Macromolecules **2007,** *40,* 1473−1479

Thiol−Allyl Ether−Methacrylate Ternary Systems. Evolution Mechanism of Polymerization-Induced Shrinkage Stress and Mechanical Properties

Tai Yeon Lee,[†] Jacquelyn Carioscia,[†] Zachary Smith,[†] and Christopher N. Bowman*,[†,‡]

Department of Chemical and Biological Engineering, University of Colorado at Boulder,
Boulder, Colorado 80309, and Dental School, University of Colorado Health Science Center,
Denver, Colorado 80045-0508

Received October 27, 2006; Revised Manuscript Received December 15, 2006

ABSTRACT: The evolution of the polymerization-induced shrinkage stress and mechanical properties of thiol−allyl ether−methacrylate ternary systems and their relationship to the polymerization kinetics have been investigated. Because of the two distinct polymerization regimes of the ternary systems—a methacrylate homopolymerization regime followed by a thiol−ene polymerization dominated regime—the mechanism for the evolution of polymerization induced shrinkage stress is unique as compared to other thiol−ene and methacrylate systems. During the first polymerization stage, only intermediate molecular weight methacrylate oligomers are produced, resulting in delayed gelation and near zero shrinkage stress. Immediately following the first polymerization stage, the allyl ether begins to polymerize, and shrinkage stress increases in correspondence with the increased allyl ether conversion. It is observed that the shrinkage stress of the ternary systems exhibits ∼50% of the shrinkage stress of the current dental restoration systems. Also, because of the two polymerization regimes, the mechanical properties evolve uniquely as compared to other ternary systems. It is noted that glass transition temperatures of the ternary systems (∼100 °C) are much higher than traditional thiol−ene polymers and comparable to the current polymeric composites for dental restorations, indicating that the thiol−allyl ether−methacrylate systems are an excellent candidate for dental restorations.

Introduction

Low polymerization-induced shrinkage and the associated stress are among the most important properties of polymeric resins for numerous applications of cross-linked polymers. Polymerization shrinkage is an almost inevitable phenomenon resulting from the reduction in molecular spacing associated with the replacement of van der Waals distances between monomers with covalent bonds in the polymer state. Shrinkage stress is then a function of both the shrinkage extent and the modulus,[1] developing only after the gel point. Therefore, the gel point, at which the material changes from a liquid monomer resin to a solid cross-linked material with a significant modulus, is an important factor in determining and controlling the shrinkage stress. Polymerization-induced shrinkage and the accompanying stress are important in several applications including dental restorative materials and electronic material coatings. One of the primary components of polymeric dental restorative materials is 2,2-bis[*p*-(3-methacryloxy-2-hydroxypropoxy)phenyl]propane (BisGMA) which is a dimethacrylate.[2,3] Methacrylate polymerizations lead to significant volume shrinkage during polymerization, 22.6 mL/mol.[4,5] Also, because of the chain growth polymerization mechanism of methacrylates, which causes the formation of high molecular weight polymers and gels at the initial stage of the polymerization, a high shrinkage stress is developed during and throughout the polymerization. One of the most deleterious effects of this shrinkage stress is debonding of the polymer/substrate interface.[6] For example, in dental restorations, shrinkage stress and the corresponding debonding and microcracking initiate microleakage between the polymer resin and tooth, resulting in secondary caries.[6]

Extensive research has been performed to reduce polymerization-induced shrinkage and stress, particularly for the multibillion dollar dental restorative industry. One focus of this research is developing BisGMA derivatives by chemically attaching bulky pendent groups to BisGMA to reduce double bond concentration.[7−9] Also, since adding low molecular weight methacrylates as a reactive diluent problematically increases volume shrinkage, researchers have developed less viscous BisGMA derivatives to avoid the use of a reactive diluent.[10−12] Further, another class of monomer systems with lower shrinkage contains hyperbranched and dendritic monomers which build upon the concept of decreasing the initial double bond concentration while simultaneously maintaining low viscosity.[13−15] One of the main research foci of low shrinkage materials is utilizing ring-opening polymerizations that decrease the amount of volume shrinkage associated with the polymerization reaction itself. For example, oxetanes,[16] oxiranes, and epoxides[17−19] are ring-opening monomers which undergo cationic polymerization proceeded by cleaving a bond of each ring to create a linear segment. This reaction exhibits lower shrinkage compared to methacrylate chain polymerization. Furthermore, research has focused on the development of expandable monomers such as spiro orthocarbonates.[20−22] Unfortunately, each of these approaches, while having promising results, has also encountered significant limitations.

Recently, thiol−ene polymerizations have been proposed as a novel approach to reduce polymerization-induced shrinkage and shrinkage stress.[5,23] Thiol−ene polymerization has many attractive advantages for both the polymerization process and ultimate material properties, including significantly reduced shrinkage and the associated stress. Reduced shrinkage and stress

---

* To whom correspondence should be addressed: e-mail: bowmanc@buffmail.Colorado.edu; Ph 303-492-3247; Fax 303-492-4341.

[†] University of Colorado at Boulder.

[‡] University of Colorado Health Science Center.

10.1021/ma0624954 CCC: $37.00

of thiol−ene polymerizations are due to the radical-mediated step growth polymerization mechanism, i.e., free radical addition followed by subsequent chain transfer.[24−26] Because of the step growth mechanism, dimers, trimers, tetramers, and oligomers are formed during the initial stage of the polymerization, resulting in significantly delayed gelation and reduced shrinkage stress as compared to (meth)acrylate systems. Also, it is reported that the volume shrinkage of thiol−ene polymerization (12−15 mL/mol) is significantly lower than methacrylate systems on a per double bond reacted basis.[5] However, one drawback of the thiol−ene polymerization is a limitation of the mechanical properties. Thiol−ene step growth polymerizations generally produce loosely cross-linked network structures as compared to (meth)acrylate systems, resulting in reduced modulus, strength, and glass transition temperature. For this reason, thiol−vinyl−vinyl ternary systems containing homopolymerizable vinyl monomers such as (meth)acrylates have been investigated.[27−29] In these systems, mixed step and chain growth polymerization occurs where the chain growth polymerization results in increased cross-link density and, hence, enhanced mechanical properties.

Previously, we indicated that thiol−allyl ether−methacrylate ternary systems exhibit two distinct polymerization regimes, and this mechanism delays gelation.[29] In this study, we have investigated the evolution mechanism of polymerization-induced shrinkage stress and mechanical properties of thiol−allyl ether−methacrylate ternary systems. On the basis of the polymerization kinetics we reported, we describe hereafter how two polymerization regimes affect the evolution process of shrinkage stress and mechanical properties.

Experimental Section

Materials. 1,6-Hexanediol dimethacrylate (90%, HDDMA) was donated by Cytec Specialty Chemicals (Smyrna, GA). Pentaerythritol tetrakis (97%, 3-mercaptopropionate) (PETMP), triethylene divinyl ether (98%, TEGDVE), and 1,3,5-triallyl-1,3,5-triazine-2,4,6(1*H*,3*H*,5*H*)-trione (98%, TATATO) were obtained from Aldrich. 2,2-Bis[4-(2-hyroxy-3-methacryloxyprop-1-oxy)phenyl]-propane (BisGMA) was donated by Esstech. The photoinitiator, 2,2-dimethoxy-2-phenylacetophenone (DMPA), was purchased from Ciba-Geigy. All monomers and the photoinitiator were used as received.

Methods. Kinetic profiles of the UV-induced polymerizations were studied using real-time FTIR, a Nicolet 750 Magna FTIR spectrometer with a KBr beam splitter and an MCT detector. Infrared spectra were recorded on a spectrometer designed to allow light to impinge on a horizontal sample using a fiber-optic cable. Monomer samples with thicknesses of about 25 μm were placed between two sodium chloride plates while the FTIR sample chamber was continuously purged with dry air. The series of infrared absorption spectra was obtained under continuous UV irradiation at a rate of 3.5 scans/s. The thiol functional group and the methacrylate double bond conversion were monitored at 2575 cm^{-1} (S−H stretching) and 816 cm^{-1} (C═C−H out of plane bending), respectively. All IR absorption peaks of allyl ether double bonds were calculated by measuring height at the shoulder of C═C−H stretching peak of the allyl ether double bond at 3081 cm^{-1}. To ensure the accuracy of the allyl ether conversion calculated in this measurement, a deconvolution technique was employed to separate an overlapping C═C stretching band of the allyl ether double bond at 3105 cm^{-1} from the methacrylate double bond at 3085 cm^{-1}. The allyl ether conversion obtained from peak height measurement was confirmed by comparing with the deconvolution results.[29] All reactions were performed under ambient conditions. Polymerizations were initiated via an EXFO Acticure light source (EXFO, Mississauga, Ontario) with a 320−500 nm filter. Irradiation intensities were measured with an International Light, Inc., model IL1400A radiometer (Newburyport, MA).

The polymerization kinetics and the shrinkage stress are simultaneously monitored using a tensometer (American Dental Association Health Foundation). The tensometer monitors shrinkage stress development using cantilever beam deflection theory. The tensile force generated by the sample shrinkage causes the cantilever beam to deflect. Deflection of the beam is translated into the appropriate stress based on the bonded sample area and the calibrated beam constant. A simultaneous kinetic profile is measured using remote near-IR transmission through the polymer sample as measured via a fiber-optic cable. A more detailed description of the measurement technique is presented elsewhere.[31] Samples were 6 mm in diameter and 1.5 mm in thickness, irradiated for 5 min, and monitored for an additional 5 min postcure. The absorption peak of the allyl ether double bonds (6130 cm^{-1}) overlaps that for the methacrylate (6165 cm^{-1}). In the near-IR, methacrylate and allyl ether double bond conversions were calculated by measuring the height of the shoulder of the C═C−H stretching overtone peaks of the allyl ether and methacrylate double bonds at 6120 and 6180 cm^{-1}, respectively. To ensure the accuracy of both double bond conversions calculated, a deconvolution technique was employed to separate the allyl ether and methacrylate double bond peaks and to calculate the conversion.

Results and Discussion

Polymerization-induced shrinkage stress is strongly affected by the cross-linked network evolution mechanism. Therefore, a fundamental understanding of the polymerization kinetics and mechanism is essential to predict the extent of polymerization-induced shrinkage stress. For example, thiol−ene polymerizations exhibit significantly reduced shrinkage stress primarily due to delayed gelation resulting from the step growth free-radical reaction mechanism. On the other hand, (meth)acrylate systems undergoing chain polymerization show higher shrinkage stress than thiol−ene systems due to early gelation at as low as 5−10% conversion.[32,33] Although thiol−ene systems exhibit low shrinkage stress with high final conversion, the mechanical properties of thiol−ene systems, especially hardness and glass transition temperature, are reduced as compared to (meth)acrylate systems. For this reason, thiol−ene−ene and thiol−ene−vinyl ternary systems have been investigated to enhance mechanical properties and controllability of the cross-linked network structure.[27−29] Hereafter, the term ene is used to designate a nonhomopolymerizable double bond such as an allyl ether, while vinyl designates a homopolymerizable double bond such as a methacrylate. In traditional thiol−ene−ene systems where neither of the vinyl groups homopolymerizes, the network evolution still occurs by a traditional step growth mechanism. On the other hand, thiol−ene−vinyl ternary systems in which one of the vinyl groups homopolymerizes exhibit a mixed chain and step growth polymerization mechanism. In this latter case, the polymerization mechanism and network structure are strongly affected by the extent of homopolymerization and the reactivity of thiyl radicals toward the two different double bonds. The thiol−allyl ether−methacrylate ternary system studied here is a thiol−ene−vinyl system which undergoes mixed chain and step growth polymerization, as reported previously.

Figure 1 presents the polymerization kinetics of pentaerythritol tetrakis(3-mercaptopropionate) (PETMP)−1,3,5-triallyl-1,3,5-triazine-2,4,6(1*H*,3*H*,5*H*)-trione (TATATO)−1,6-hexanediol dimethacrylate (HDDMA) mixtures. The HDDMA content is 50 wt % while the allyl ether and thiol functional group ratio (TATATO/PETMP) is maintained at 1:1. As described in our previous report, the thiol−allyl ether−methacrylate mixtures exhibit two distinct polymerization regimes: a methacrylate homopolymerization dominated regime with significant chain transfer to thiol followed by a thiol−ene polymerization dominated regime.[29] During the initial poly-

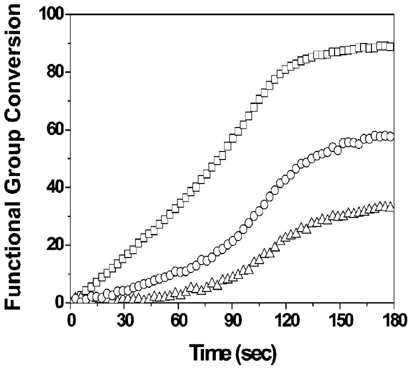

Figure 1. Functional group conversion vs time for a PETMP−TATATO−HDDMA ternary mixture: methacrylate (□), thiol (○), and allyl ether (△) conversion. HDDMA content is 50 wt %, and the TATATO/PETMP functional group ratio is 1:1. Samples contain 0.1 wt % DMPA and are irradiated at 15 mW/cm^2 using 320−500 nm light.

merization stage (up to 40−50% methacrylate conversion), TATATO does not polymerize to any significant extent while the HDDMA double bond conversion increases rapidly. Because the thiol functional group conversion increases slowly during this stage, it is expected that methacrylate radicals undergo a chain transfer reaction to the thiol. On the basis of this result, it is presumed that thiyl radicals produced by the chain transfer reaction of methacrylate radicals to thiol functional groups do not react to a significant extent with allyl ether double bonds during this stage. After a significant amount of methacrylate double bonds have polymerized, the allyl ether undergoes thiol−ene polymerization. Details of the polymerization kinetics of the ternary system are described in our previous report.[29]

As shown in Figure 1, the distinct polymerization regimes of the thiol−allyl ether−methacrylate systems result in a unique network evolution process. Figure 2 presents an illustration of the network evolution based on the two different polymerization regimes. From the homogeneous mixture of thiol, allyl ether, and methacrylate monomers, low molecular weight methacrylate oligomers, terminated by the chain transfer reaction to thiol or end-capped with thiol monomers from the addition of thiyl radicals to methacrylate double bonds, are produced during the initial stage of polymerizations. As described in our previous report, the molecular weight of the methacrylate oligomers decreases with increasing thiol content because of an increase in the chain transfer rate. During this stage, the allyl ether does not participate in the polymerization reaction and effectively acts as a diluent. Therefore, it is presumed that no gelation occurs during this stage. Following this stage, the allyl ether begins to react with the thiol functional group, producing cross-linked networks (gelation) and resulting in the evolution of polymerization-induced shrinkage stress. On the basis of this network evolution process, it is expected that shrinkage stress of the ternary systems is delayed and ultimately lower than (meth)acrylate systems.

To evaluate the evolution mechanism of the polymerization-induced shrinkage stress in this ternary system, the shrinkage stress and double bond conversion of methacrylates, thiol−ene, and thiol−allyl ether−methacrylate systems are plotted as a function of polymerization time in Figure 3. Thiol−ene and methacrylate systems were studied as controls or standard samples for comparison with the ternary system. The BisGMA/TEGDMA 70/30 (wt %) mixture corresponds to currently used dental resins, and the PETMP/TATATO mixture is the thiol−

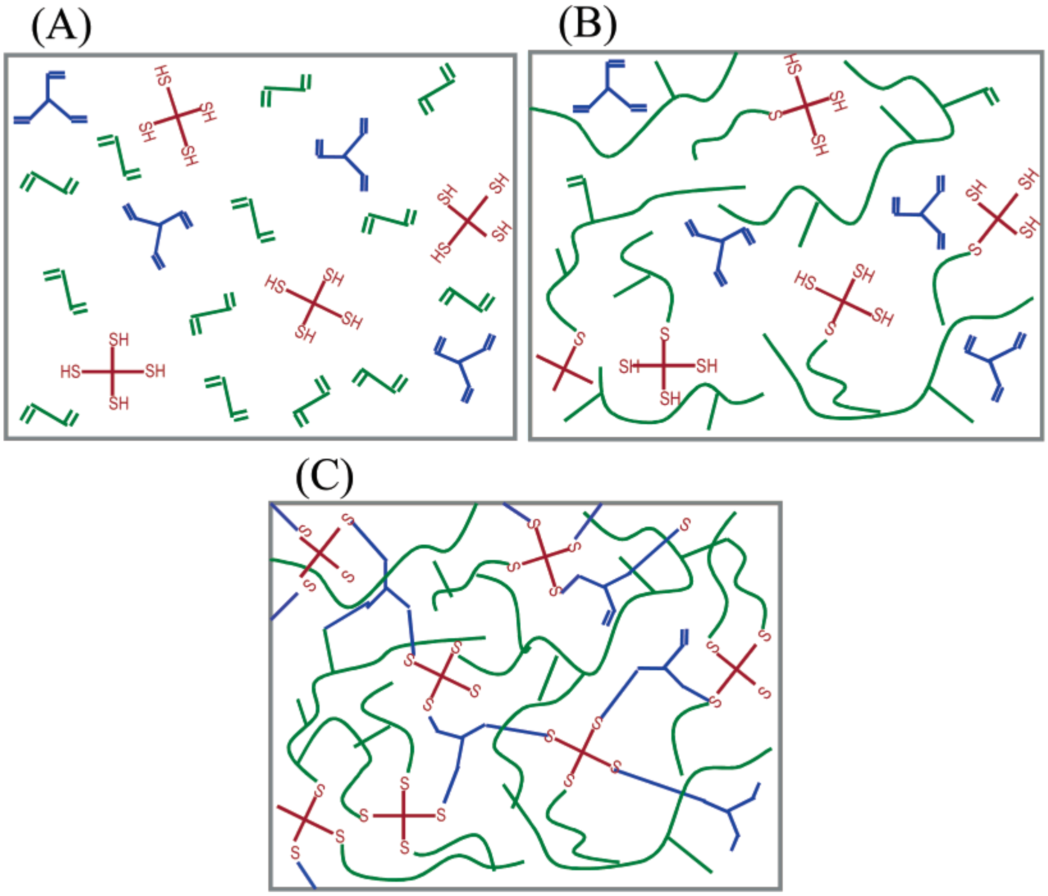

Figure 2. A diagram illustrating the network evolution mechanism of thiol−allyl ether−methacrylate ternary systems: (A) before polymerization, (B) first polymerization regime, and (C) second polymerization regime.

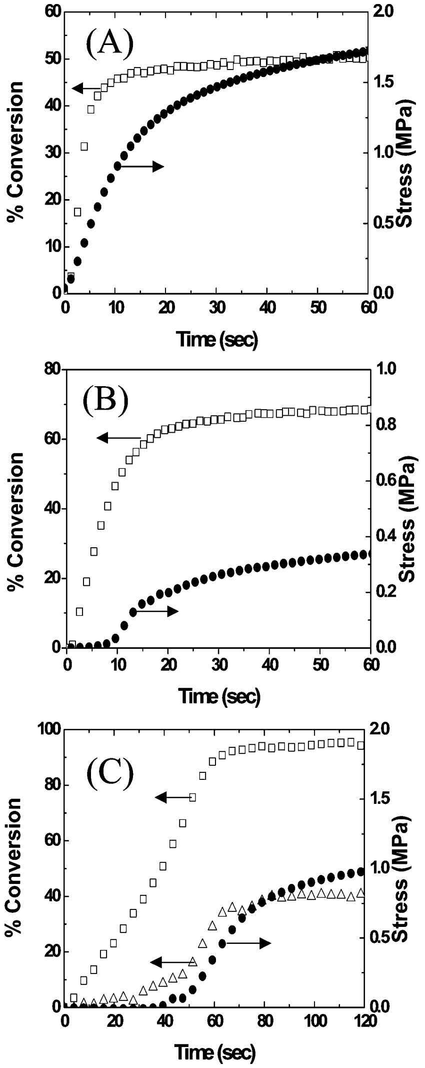

Figure 3. Polymerization-induced shrinkage stress and double bond conversion of (A) BisGMA/TEGDMA 70/30, (B) PETMP−TATATO, and (C) PETMP−TATATO−HDDMA (HDDMA 50 wt %) as a function of polymerization time: methacrylate (□) and TATATO (△) conversion and shrinkage stress (●). Samples A and C contain 0.1 wt % DMPA and are irradiated at 15 mW/cm^2, and sample B contains 0.05 wt % DMPA and are irradiated at 5 mW/cm^2 using 320−500 nm light.

ene formulation which exhibits the highest glass transition temperature among commercially available thiol−ene formulations. As shown in Figure 3a, polymerization-induced shrinkage stress is almost immediately developed upon polymerization of the methacrylate due to the low gel point. In the thiol−ene system, shrinkage stress is significantly lower than the methacrylate system due to delayed gelation resulting from the step growth polymerization mechanism. The volume shrinkage that occurred prior to the gel point does not result in shrinkage stress development because viscous liquid flow accommodates the shrinkage without leading to stress development. The thiol and ene monomers used in this study are tetra- and trifunctional, respectively. In this case, the gelation occurs at ~40% functional group conversion. As shown in Figure 3b, thiol−ene polymerization shows nearly zero shrinkage stress until ~40% conversion, and then the stress increases. Like the thiol−ene system, the thiol−allyl ether−methacrylate system exhibits a unique shrinkage stress evolution process, as shown in Figure 3c. The shrinkage stress does not increase until 40 s, by which time the methacrylate conversion is ~50%. The stress begins to develop right before the allyl ether starts to polymerize. This result indicates that there is no shrinkage stress development during the first polymerization regime. Thus, no gelation occurs during the first polymerization regime dominated by methacrylate homopolymerization with significant chain transfer to thiol. In the second regime, the allyl ether polymerizes with the thiol functional groups and increases conversion rapidly and dramatically. Correspondingly, the shrinkage stress increases rapidly with allyl ether conversion at this stage. This result indicates that during the second polymerization regime cross-linked networks are formed and gelation occurs. This result strongly supports the proposed polymerization mechanism and network structural evolution process illustrated in Figures 1 and 2, respectively.

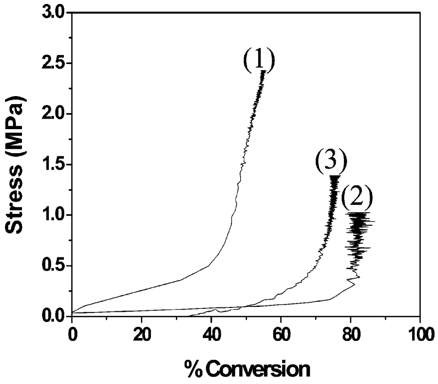

Figure 4. Shrinkage stress of (1) BisGMA/TEGDMA 70/30, (2) PETMP−TATATO, and (3) PETMP−TATATO−HDDMA (HDDMA 50 wt %) as a function of the overall double bond conversion. Standard deviations are ±0.16, ±0.13, and 0.09 MPa for the samples 1, 2, and 3, respectively. Samples contain 0.1 wt % DMPA and are irradiated at 15 mW/cm^2 using 320−500 nm light.

The delayed gelation of the thiol−allyl ether−methacrylate system also results in lower ultimate shrinkage stress. Figure 4 presents the shrinkage stress of the above three systems as a function of the total double bond conversion. The final shrinkage stress of the methacrylate system (BisGMA/TEGDMA 70/30) reaches 2.5 ± 0.2 MPa while the thiol−ene system exhibits a final stress of ~1 ± 0.1 MPa under these conditions. This difference arises because of the delayed gelation of the thiol−ene polymerization as explained previously. The ultimate shrinkage stress of the ternary system is ~1.3 ± 0.2 MPa, which is half of the final stress of the methacrylate system and nearly that of the thiol−ene system. If the final stress value is normalized by the functional group conversion, the normalized final stress of the thiol−ene and the ternary systems are 3.5 and 2.5 times lower than that of the methacrylate system, respectively. In addition to providing supporting evidence on two separate polymerization mechanisms of the ternary system, this result also suggests that the thiol−allyl ether−methacrylate systems exhibit significantly delayed gelation and reduced polymerization induced shrinkage stress during polymerization. The reduced stress of the thiol−allyl ether−methacrylate systems is of great interest for applications requiring low shrinkage stress such as electronic material coatings and polymeric resins for dental restorations.

The reduced shrinkage stress of the ternary system is primarily due to the polymerization kinetics that result in delayed gelation. Examining the dark polymerization kinetics provides further supporting evidence that gelation does not occur during the first polymerization regime. When the initiating light source is turned off during the first stage, the polymerizations immediately cease because the radicals rapidly terminate due to higher mobility. In the second stage, when the initiating light is turned off, the polymerization continues for a time in the dark, indicative of

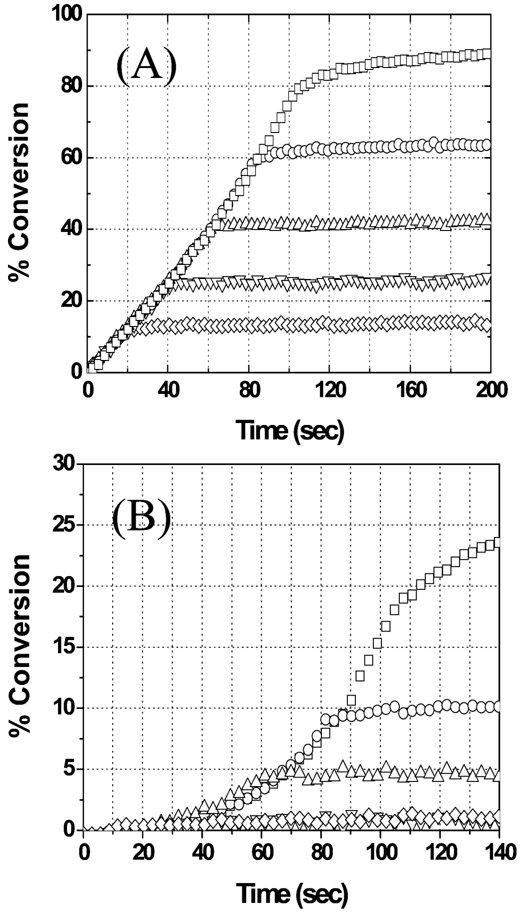

Figure 5. Functional group conversions of (A) methacrylate and (B) allyl ether double bonds of PETMP−TATATO−HDDMA ternary systems during dark polymerization. UV light is cut off after 20 (◇), 40 (▽), 60 (△), 80 (○), and 100 s (□). HDDMA content is 50 wt %, and the TATATO/PETMP functional group ratio is 1:1. Samples contain 0.1 wt % DMPA and are irradiated at 15 mW/cm^2 using 320−500 nm light.

reduced mobility associated with the network development. Figure 5 presents methacrylate and allyl ether conversions of the PETMP−TATATO−HDDMA ternary mixture during dark polymerization reactions. The HDDMA content is 50 wt %, and the thiol/allyl ether functional group ratio is maintained at 1:1. The polymerizations are stopped at 20, 40, 60, 80, and 100 s after initially turning the light on. It is clearly seen that only minimal conversion of both methacrylate and allyl ether double bonds occurs when the UV light is turned off after 20, 40, and 60 s of polymerization. When polymerization is stopped after 80 s of UV irradiation, both methacrylate and allyl ether double bonds continue to react during the dark polymerization period. Approximately 5% and 25% increases in the double bond conversion are observed during the dark polymerization period when the polymerizations are stopped at 80 and 100 s, respectively. This result indicates that the mobility in the system decreases significantly after the first polymerization regime. Only after the allyl ether begins to polymerize, during the early portion of the second polymerization stage, does dark polymerization occur. It should be noted that pure methacrylate systems exhibit significant dark polymerization even when polymerizations are stopped near 5−10% conversion.[31] This result is consistent with the proposed shrinkage stress development mechanism of the ternary systems.

Further studies on the shrinkage stress of the ternary system containing BisGMA as a methacrylate component provide information about whether the thiol−allyl ether−methacrylate ternary systems are appropriate as polymeric resins for dental restoration. When BisGMA is used as the methacrylate in the ternary system, the glass transition temperature of the ternary mixtures becomes comparable to the T_g of the current BisGMA/TEGDMA 70/30 mixture (as discussed later). Figure 6 illustrates the shrinkage stress and double bond conversion of a PETMP−TATATO−BisGMA ternary mixture. The BisGMA content is 50 wt %, and the PETMP/TATATO ratio is 1:1.4. Because the thiol peak is not measurable for this system with the NIR technique, only the two double bond conversions are plotted along with the shrinkage stress. The same polymerization tendency is observed as shown in Figure 3c. After 40−50% of BisGMA double bonds polymerize, the thiol−allyl ether begins to polymerize, exhibiting the same polymerization regimes observed previously.

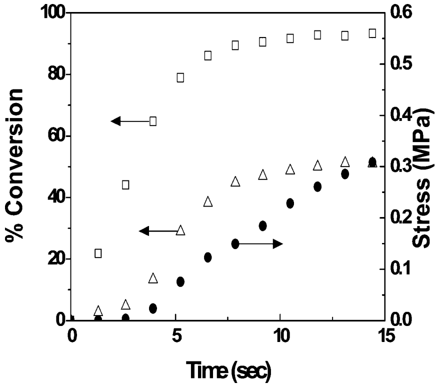

Figure 6. Polymerization-induced shrinkage stress and double bond conversion of PETMP−TATATO−BisGMA (BisGMA 50 wt %) as a function of polymerization time: methacrylate (□) and TATATO (△) conversion and shrinkage stress (●). Samples contain 0.1 wt % DMPA and are irradiated at 15 mW/cm^2 using 320−500 nm light.

The shrinkage stress as a function of the methacrylate, allyl ether, and total double bond conversion of the PETMP−TATATO−BisGMA ternary mixture is presented in Figure 7. As expected from the polymerization kinetics, the final shrinkage stress is significantly reduced as compared to the BisGMA/TEGMA system. For the sample containing 50 wt % BisGMA, the shrinkage stress does not begin to develop until 50% methacrylate double bond conversion while the stress begins to increase after 30−35% methacrylate conversion in the sample containing 70 wt % BisGMA. With increasing BisGMA content, chain transfer of methacrylate radicals to thiols decreases, resulting in the formation of a cross-linked network at lower methacrylate conversion. Also, the shrinkage stress of the sample containing 50 wt % of BisGMA gradually increases with increasing TATATO conversion up to 45%. On the other hand, the shrinkage stress increases rapidly with increasing TATATO conversion for the sample containing 70 wt % BisGMA. With increasing BisGMA content (70 wt % BisGMA), higher molecular weight methacrylate oligomers capped with thiol functional groups are produced during the first polymerization regime. In this case, gelation occurs significantly earlier because the system contains higher molecular weight multifunctional methacrylates and thiol oligomer. When relatively low molecular weight methacrylate oligomers capped with thiol functional groups are formed in the first polymerization stage (50 wt % BisGMA), gelation is delayed compared to the sample containing 70 wt % BisGMA. Even with early gelation of the sample containing 70 wt % BisGMA, the ultimate shrinkage stress values of both samples are approximately the same (1.1 ± 0.1 and 1.1 ± 0.2 MPa for 50 and 70 wt % BisGMA content, respectively). This outcome is due to the lower double bond

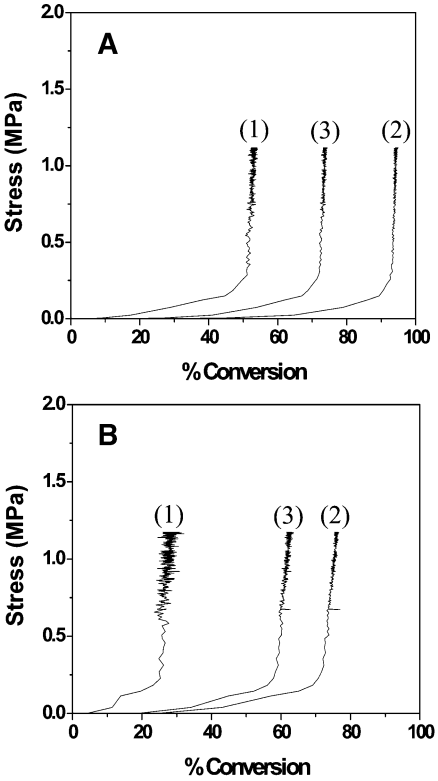

Figure 7. Shrinkage stress of PETMP−TATATO−BisGMA mixtures as a function of (1) TATATO, (2) BisGMA, and (3) total conversion for the samples that contain 50 (A) and 70 wt % (B) BisGMA with the reminder containing a 1:1 molar ratio of thiol to allyl ether functional groups. Standard deviations are ±0.08 MPa and ±0.2 for 50 and 70 wt % BisGMA content, respectively. Samples contain 0.1 wt % DMPA and are irradiated at 15 mW/cm^2 using 320−500 nm light.

conversion of the sample with the higher BisGMA content. If the final shrinkage stress is normalized by the total double bond conversion, the shrinkage stress of the 70 wt % BisGMA sample is ∼30% higher than for the 50 wt % BisGMA sample.

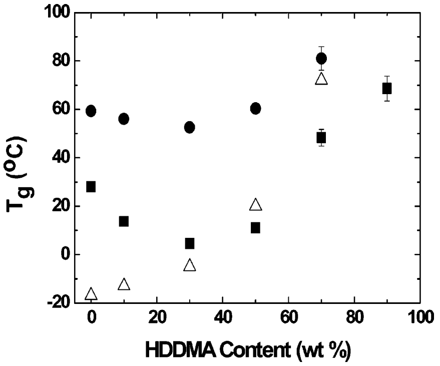

Figure 8. Glass transition temperature (T_g) of HDT−TATATO−HDDMA (■), PETMP−TATATO−HDDMA (●), and PETMP−TEGDVE−HDDMA (△) mixtures as a function of the methacrylate content (wt %).

In addition to polymerization-induced shrinkage stress, the unique two polymerization regimes of the ternary system affect mechanical properties. In a previous report, we described the effect of the thiol functionality on the glass transition temperature and the rubbery storage modulus. Both properties significantly increase with increasing thiol functionality. Because of the significant effect of the thiol content on the polymerization kinetics as shown in Figure 7 and the previous report, it is expected that the mechanical properties and network structure of cured materials are altered by changing the thiol concentration. In fact, the mechanical properties of the thiol−allyl ether−methacrylate ternary systems, as a function of thiol content, are affected by several factors. As explained previously, the methacrylate chain length decreases dramatically with increasing thiol content. However, it is also notable that the conversion of methacrylate, allyl ether, and thiol functional groups increase with increasing thiol content. Reduced methacrylate chain length decreases the cross-link density while enhancing the final conversion of the three functional groups increases the cross-link density. Also, as methacrylates exhibit higher glass transition temperatures than thiol−enes, increasing the methacrylate content enhances the T_g of the thiol−allyl ether−methacrylate mixtures. Figure 8 shows the glass transition temperature of the thiol (HDT or PETMP)−TATATO−HDDMA mixtures as a function of thiol−ene content. As expected, T_g increases with increasing methacrylate content. However, an interesting result is observed when more than 70 wt % thiol−ene is incorporated. A minimum T_g is observed at 70 wt % thiol−ene content, and then the T_g increases with further increases of the thiol−ene content. The increase of T_g with increasing HDDMA content is explained by the increase of the higher T_g component (HDDMA), relatively long methacrylate chain length, and the high cross-link density due to limited chain transfer to thiol although HDDMA conversion decreases. With decreasing HDDMA content, chain transfer to thiol reduces the cross-link density and, hence, T_g. The samples containing more than 70 wt % thiol−ene exhibit a T_g increase likely due to the limited HDDMA content. The presence of even 10 wt % of HDDMA obviously has a detrimental effect on the mechanical properties of the pure thiol−ene.

The second thiol−ene−ene ternary system, the thiol−vinyl ether−methacrylate mixture, exhibits different polymerization kinetics as compared to the thiol−allyl ether−methacrylate systems.[29] It is expected that the different polymerization mechanism must have a different effect on the mechanical properties. Figure 8 also shows the T_g change of the PETMP−TEGDVE−HDDMA mixtures as a function of the thiol−ene content. Interestingly, T_g increases with HDDMA content continuously. It is expected that in the thiol−vinyl ether−methacrylate systems the effect of the chain transfer reaction on the cross-linked network structure and mechanical properties increases continuously with increasing thiol−ene content. On the other hand, in the thiol−allyl ether−methacrylate systems, this effect does not continuously increase with increasing thiol−ene content because of the two different polymerization stages.

When BisGMA is used instead of HDDMA, enhanced mechanical properties of the thiol−allyl ether−methacrylate ternary system are obtained. The highest obtainable T_g from the PETMP−TATATO−HDDMA mixtures is ∼80 °C. Figure 9 presents the tangent δ as a function of temperature for the PETMP−TATATO−BisGMA mixtures. The T_g of the ternary sample containing 50% of BisGMA is ∼83 ± 2 °C, comparable to the highest T_g of the PETMP−TATATO−HDDMA mixtures. Interestingly, the ternary sample containing 70 wt % BisGMA exhibits two peak maxima at 90 ± 3 and 115 ± 4 °C. This result is primarily due to the low TATATO and thiol conversion in this sample and the associated continuing reaction. When the sample is reheated, the T_g increases significantly (130 ± 4 °C), and only one peak is observed. This value is higher than the T_g of a BisGMA/TEGDMA 70/30 mixture. This increase is due to the reaction between unreacted thiol and allyl ether functional groups during the first heating cycle, resulting in increased cross-link density. Upon heating, the trapped radicals present in the sample initiate the polymerization of unreacted

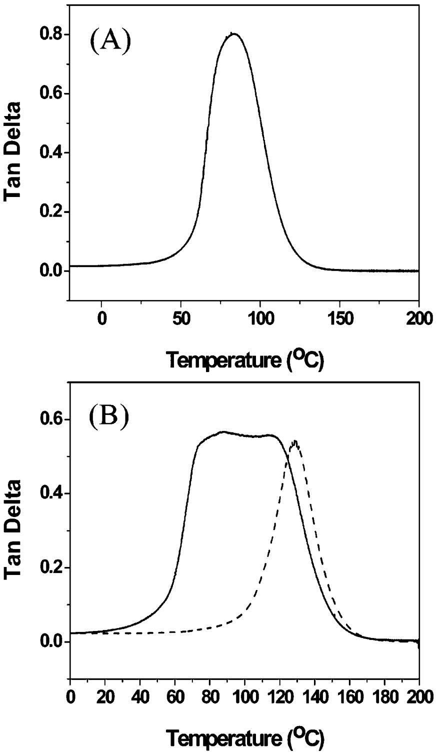

Figure 9. DMA tangent δ curve of PETMP−TATATO−BisGMA mixtures containing 50 (A) and 70 wt % BisGMA (B) for both the first (line) heating cycle and for the second (dotted line) heating cycle.

functional groups due to increased chain mobility. In addition to increased T_g, the peak width of the tangent δ curve is significantly narrower as compared to methacrylates. The peak width of the sample shown in Figure 9b is 64 ± 5 and 30 ± 3 °C for the first and second cycles, respectively. As previously reported, a BisGMA/TEGDMA 70/30 mixture, as well as most highly cross-linked dimethacrylates, exhibits a peak width broader than 100 °C. This result indicates that the thiol−allyl ether−methacrylate ternary system produces materials with higher T_g and more homogeneous network structures as compared to methacrylate systems. Obtaining a homogeneous structure is ideal for tuning material properties to specific applications.

Conclusion

The evolution process of polymerization-induced shrinkage stress and mechanical properties of thiol−allyl ether−methacrylate ternary systems has been investigated on the basis of extensive knowledge of the polymerization kinetics. Two distinct polymerization stages—methacrylate homopolymerization with extensive chain transfer to thiol followed by a nearly ideal thiol−ene reaction—significantly influence the shrinkage stress and mechanical property evolution. During the first stage, shrinkage stress does not develop because gelation does not occur since only oligomeric, highly functional methacrylates are formed. During the second polymerization stage, the allyl ether conversion and shrinkage stress increase simultaneously as indicative of gelation. This behavior results in significantly reduced shrinkage stress comparable to traditional thiol−ene systems while having the benefit of higher cross-linking density and improved mechanical properties. Because methacrylate homopolymerization with chain transfer to thiols dominates the first polymerization regime, the initial thiol concentration has a dramatic effect on the glass transition temperature and other properties. Ultimately, this work shows that thiol−allyl ether−methacrylate ternary systems have significant potential for the development of high-performance polymeric resins with low shrinkage stress and enhanced mechanical properties comparable to methacrylates.

Acknowledgment. The authors acknowledge the NSF Industry/University Cooperative Research Center for Fundamentals and Applications of Photopolymerizations for funding of this work.

References and Notes

(1) Stansbury, J. W. *Dent. Mater.* **2005**, *21*, 56.
(2) Bowen, R. L. US Patent 3,066,122, 1962.
(3) Moszner, N.; Salz, U. *Prog. Polym. Sci.* **2001**, *26*, 535.
(4) Patel, M. P.; Braen, M.; Davy, K. W. M. *Biomaterials* **1987**, *8*, 53.
(5) Lu, H.; Carioscia, J. A.; Stansbury, J. W.; Bowman, C. N. *Dent. Mater.* **2005**, *21*, 1129.
(6) Davison, C. L.; Feilzer, A. J. *J. Dent.* **1997**, *25*, 435.
(7) Chung, C. M.; Lee, S. J.; Lim, J. G.; Jang, D. O. *J. Biomed. Mater. Res.* **2002**, *62*, 622.
(8) Kim, Y.; Kim, K. C.; Cho, B. H.; Son, H. H.; Um, C. M.; Kim, O. Y. *J. Biomed. Mater. Res., Part B: Appl. Biomater.* **2004**, *70B*, 82.
(9) Dulik, D.; Bernier, R.; Brauer, G. M. *J. Dent. Res.* **1981**, *60*, 983.
(10) Pereira, S. G.; Osorio, R.; Toleano, M.; Nunes, T. G. *Dent. Mater.* **2005**, *21*, 823.
(11) Kalachandra, S.; Sankarapandian, M.; Shobha, H. K.; Taylor, D. F.; McGrath, J. E. *J. Mater. Sci.: Mater. Med.* **1997**, *8*, 283.
(12) Pereira, S. G.; Nunes, T. G.; Kalachandra, S. *Biomaterials* **2002**, *23*, 3799.
(13) Klee, J. E.; Walz, U.; Holter, D.; Frey, H.; Mulhaupt, R. *Angew. Makromol. Chem.* **1998**, *260*, 71.
(14) Klee, J. E.; Schneider, C.; Holter, D.; Burgath, A.; Frey, H.; Mulhaupt, R. *Polym. Adv. Technol.* **2001**, *12*, 346.
(15) Grohn, F.; Kim, G.; Bauer, A. J.; Amis, E. J. *Macromolecules* **2001**, *34*, 2179.
(16) Nuyken, O.; Bohner, R.; Erdmann, C. *Macromol. Symp.* **1996**, *107*, 125.
(17) Chappelow, C. C.; Pinzino, C. S.; Power, M. D.; Holder, A. J.; Morrill, J. A.; Jeang, L. *J. Appl. Polym. Sci.* **2002**, *86*, 314.
(18) Eick, J. D.; Kostoryz, E. L.; Rozzi, S. M.; Jacobs, D. W.; Oxman, J. D.; Chappelow, C. C. *Dent. Mater.* **2002**, *18*, 413.
(19) Tilbrook, D. A.; Clarke, R. L.; Howle, N. E.; Braden, M. *Biomaterials* **2000**, *21*, 1743.
(20) Moon, E. J.; Lee, J. Y.; Kim, C. K.; Cho, B. H. *J. Mater. Sci.: Mater. Med.* **1997**, *8*, 283.
(21) Hino, T.; Endo, T. *Macromolecules* **2003**, *36*, 338.
(22) Bromley, M. K.; Solomon, D. H. *Polymer* **1999**, *40*, 6539.
(23) Carioscia, J. A.; Lu, H.; Stanbury, J. W.; Bowman, C. N. *Dent. Mater.* **2005**, *21*, 1137.
(24) Jacobine, A. F. In *Radiation Curing in Polymer Science and Technology III, Polymerisation Mechanisms*; Fouassier, J. D., Rabek, J. F., Eds.; Elsevier Applied Science: London, 1993; Vol. 3, p 219.
(25) Hoyle, C. E.; Lee, T. Y.; Roper, T. *J. Polym. Sci., Part A: Polym. Chem.* **2004**, *42*, 5301.
(26) Morgan, C. R.; Magnotta, F.; Ketley, A. D. *J. Polym. Sci., Polym. Chem. Ed.* **1977**, *15*, 627.
(27) Reddy, S. K.; Cramer, N. B.; Bowman, C. N. *Macromolecules* **2006**, *39*, 3681.
(28) Reddy, S. K.; Cramer, N. B.; Kalvaitas, M.; Lee, T. Y.; Bowman, C. N. *Aust. J. Chem.* **2006**, *59*, 586.
(29) Lee, T. Y.; Smith, Z.; Reddy, S. K.; Bowman, C. N. *Macromolecules*, in press.
(30) Lee, T. Y.; Roper, T. M.; Jonsson, E. S.; Kudyakov, I.; Viswanathan, K.; Nason, C.; Guymon, C. A.; Hoyle, C. E. *Polymer* **2003**, *44*, 2859.
(31) Lu, H.; Stansbury, J. W.; Dickens, S. H.; Eichmiller, F. C.; Bowman, C. N. *J. Biomed. Mater. Res., Part B: Appl. Biomater.* **2004**, *70B*, 206.
(32) Anseth, K. S.; Wang, C. M.; Bowman, C. N. *Macromolecules* **1994**, *27*, 650.
(33) Tryson, G. R.; Shultz, A. R. *J. Polym. Sci., Polym. Phys. Ed.* **1979**, *17*, 2059.

MA0624954